Research Statement

Uday Mathur
Department of Physics, Indian Institute of Technology (BHU), Varanasi

Physics seeks to predict and quantify natural events using mathematics, and recent advances hint at a fundamental, purely mathematical basis for the universe—a concept that has always fascinated me. I am particularly drawn to phenomena with clear mathematical foundations, like the differential equation of a damped harmonic oscillator, which aligns with both intuition and observation. Quantum mechanics, however, delves even deeper into this realm, where mathematical constructs define everything we can know about physical entities, often with little intuitive guidance. My interest in quantum computation stems from this desire to explore the boundary where mathematics and physical reality converge. I am unwavering in my commitment to rethinking and expanding our understanding of the world through this lens.

During my summer break, under the guidance of Dr.Rajeev Singh[1], I worked on a paper [1] based on quantum hardware and devices, by Zlatko K. Minev. The paper introduces the Energy Participation Ratio (EPR) method, which quantizes circuits by determining how much of a mode's energy is stored in each element. The paper extensively explored the EPR's application across many devices. To be concise, I will focus on the EPR-related data generated by me for three major devices: ***Configuration A***, ***Configuration B*** and ***Flip-Chip*** [2]. Our primary objective was to fine-tune a quantum device to achieve the desired Hamiltonian, $\hat{H}_{\text{full}}$.

As a first step, I have designed the devices mentioned earlier using ***Qiskit-Metal*** [3]. Then after analysis and optimizing the device parameters, I used ***Ansys high-frequency electromagnetic-field simulator*** **(HFSS)** [4] for FE analysis, specifically Eigenmode analysis for the mentioned devices. Then I used an open-source library named **pyEPR** [5] to extract the participation ratios. I have obtained the data related to the device shown in Table 1 and Table 2, all device dimensions of the devices had to be estimated, they were not mentioned in the paper. I made the devices both in *Ansys* and *Qiskit-metal* however have considered *Ansys HFSS* design for better results.

The *energy-participation ratio* p_{mj} of junction j in eigenmode m is the fraction of inductive energy stored in the junction when only that mode is excited. It plays the primary role in the construction of the system many-body Hamiltonian

$$p_{mj} := \frac{\text{Inductive energy stored in junction } j}{\text{Inductive energy stored in mode } m}$$

Here, we consider a general nonlinear device, a Josephson dipole as a lumped two-terminal flux-controlled element. It possesses a characteristic energy function that encapsulates all details of its constitution $\varepsilon_j(\varphi_j)$. Its energy function can be conceptually separated into two parts as shown below

$$\varepsilon_j(\Phi_j) = \varepsilon_j^{\text{lin}}(\Phi_j) + \varepsilon_j^{\text{nl}}(\Phi_j) \tag{1}$$

[1]Assistant Professor, Department of Physics, IIT-BHU, Varanasi

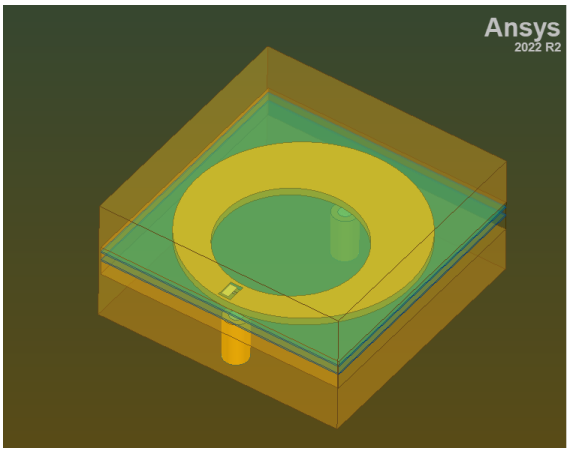

Figure 1: **Illustration of flip-chip device**

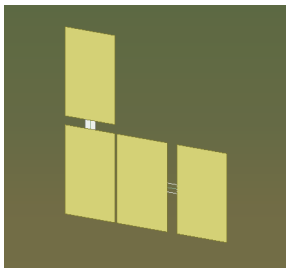

(a) **Configuration-A**

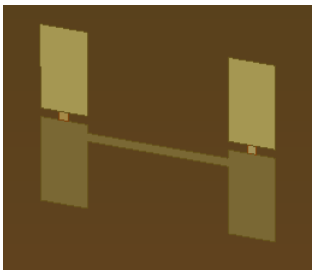

(b) **Configuration-B**

Here Φ_j is generalized flux across the device terminals where j denotes the j-th Josephson dipole in the circuit. $\varepsilon_j^{\text{lin}}(\Phi_j)$ signifies all the terms associated with the linear response of the dipole and $\varepsilon_j^{\text{nl}}(\Phi_j)$, with non-linear terms.

Similarly we can write the corresponding Hamiltonian of the Josephson circuit consisting of EM and Josephson elements

$$\hat{H}_{full} = \hat{H}_{lin} + \hat{H}_{nl} \tag{2}$$

Here the quantized linear Hamiltonian of the linearized Josephson circuit can be expressed as

$$\hat{H}_{lin} = \sum_{m \in M} \hbar w_m \hat{\alpha}_m^\dagger \hat{\alpha}_m \tag{4}$$

while its non-linear part is

$$\hat{H}_{nl} \equiv \sum_{j \in J} \varepsilon_j^{nl} = \sum_{j \in J} \sum_{p=3}^{\infty} E_j c_{jp} \hat{\varphi}_j^p \tag{3}$$

where E_j is an overall scaling factor of the energy function, c_{jp} an *dimensionless* coefficient. M is a set of modes, w_m is the solution eigenfrequency of mode m and $\hat{\alpha}_m$ is the m-th mode amplitude (annihilation operator). On further calculation it can be shown that the values ϕ_{mj} and p_{mj} are related as

$$\phi_{mj} = S_{mj} \sqrt{p_{mj} \hbar w_m / 2E_j} \tag{4}$$

From here we can define a vector EPR by the components $\{S_{mj}\sqrt{p_{mj}} | m = 1, ..., M\}$ where $S_{mj} = +1$ or $S_{mj} = -1$ is the EPR *sign bit* of Josephson device j in mode m. For a

device with multiple junctions, the EPR of junction j in the m-th mode is calculated as

$$p_{mj} = \frac{1}{2} L_j I_{mj}^2 / \varepsilon_{ind} \tag{5}$$

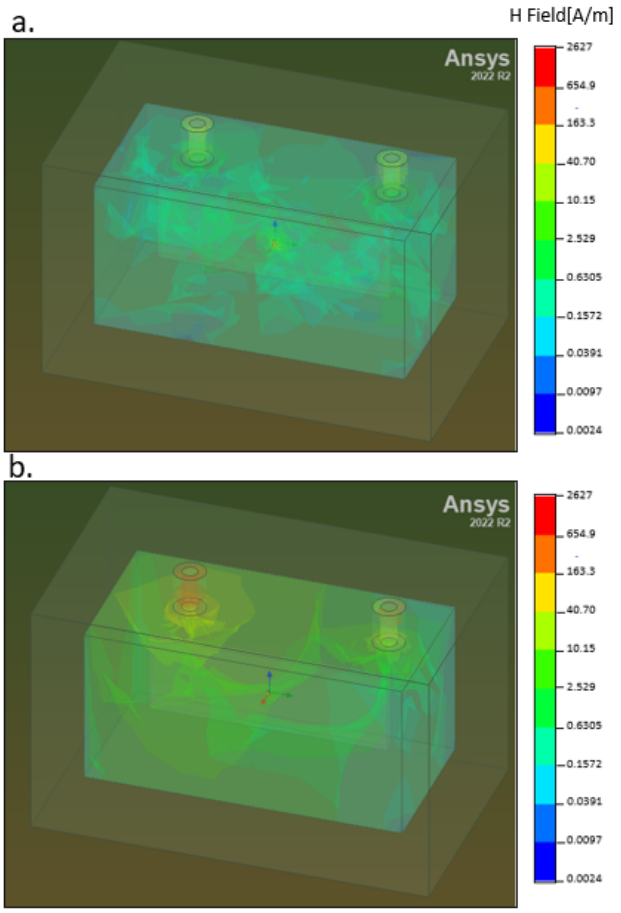

Figure 3: (a) Eigenmode simulation of qubit mode and (b) Eigenmode simulation of cavity mode of *Configuration-A device*

The above two figures represent the eigenmode simulations of **Qubit mode** and **Cavity mode** of *Configuration-A* device. I performed the **H-field simulation** in Ansys HFSS and came up with two types of H-field patterns. When mode 1 is excited, the field pattern shows the Qubit mode as shown in Figure 3(a), the electric field will be stronger near the Josephson junction and weaker elsewhere. On the other hand, on excitation of mode 2, the field pattern shows cavity mode as shown in Figure 3(b), the field distribution concentrated within the cavity structure, with little interaction with the qubit. I used the normalization factor of 10^{-12} for the H field measurement scale. I also produced these modes for *Configuration-B* device and *flip-chip device*, although I mentioned a small amount of useful data for both *Configuration A* and *B* devices.

Here I only discussed the qubit and cavity mode, ignoring the hybridized mode between cavity and qubit. However, both, *Configuration-A* and *Configuration-B* devices are in strong coupling with a cavity ($g >> \Delta$), where g is coupling strength and Δ is detuning, the difference between cavity mode and qubit mode frequency. Here I have mentioned the data of EPR analysis of devices.

Table 1: EPR analysis data of *Configuration-A*

Parameters	*Mode 1(Qubit mode)*	*Mode 2(Cavity mode)*
w**(GHz)**	5.150437	6.138809
p_{j_1}	0.703529	0.265410
p_{j_2}	0.132536	0.347030
Q_f	4.287381x10^7	1.574372x10^7
S_{j_1}	-1	-1
S_{j_2}	+1	-1

For the data in Table 1 of *Configuration-A* device, I had set the distance between the lower pad of vertical qubit and left pad of horizontal qubit (**Trans_gap**), to 0.01 mm, this is an essential parameter, as it varies the S_{21} vs frequency (GHz) graph, which helps in determining the type of coupling (weak coupling or strong coupling), the qubit system has with the cavity.

Table 2: EPR analysis data of *Configuration-B*

Parameters	*Mode 1(Cavity mode*	*Mode 2(Qubit Mode)*
w **(GHz)**	7.209611	10.462019
p_{j_1}	0.475722	0.463047
p_{j_2}	0.482649	0.457023
Q_f	3.633531×10^8	6.170478×10^5
S_{j_1}	+1	-1
S_{j_1}	-1	-1

In Table 2, I represent the data that I have extracted for **configuration-B** device. Here also I ignored the hybridization of the modes, although it has a slightly strong coupling between qubit and cavity system as its $g > \Delta$. I calculated g using *Vacuum Rabi oscillation* frequency formula ($g = 1/2\sqrt{(\Delta w)^2 - \Delta^2}$), and calculated Δw using S_{21} v/s Frequency graph. I analyzed Energy participation-related data, quality factor, and S parameter graph and predicted the coupling the devices have with a cavity.

Additionally I have also been learning quantum algorithms and programming quantum circuits to run on a real-time quantum computer using IBM's Qiskit. My recent work includes labs[6] completed under **Qiskit Global Summer School 2024**. Attached herewith is the validation for your reference [7].

My current work is focused on the theory of quantum circuits and reproducing another research paper on ***Unveiling photon-photon coupling induced transparency and absorption***[8] which has pushed me into the domain of ***Hybrid Quantum systems*** and is exposing me to another simulation software such as **CST Studio** for designing, analyzing and optimizing EM components. The paper discusses the theoretical foundations of coupling-induced transparency (CIT) and absorption (CIA), respectively, and explores the transition between these phenomena. I am new to this field so I am still exploring new concepts, the potential applications and advancements in this area excite me and I am committed to contributing to the field.

References

[1] Zlatko K. Minev et al., "Energy-participation ratio of Josephson circuits", *Physical Review Applied*, vol. 15, no. 3, pp. 034057, March 2021.

[2] Z. K. Minev, I. M. Pop, and M. H. Devoret, "Planar Superconducting Whispering Gallery Mode Resonators," *Appl. Phys. Lett.*, vol. 103, p. 142604, 2013. [Online]. Available: `https://doi.org/10.48550/arXiv.1308.1743`.

[3] Qiskit Metal: An open-source framework for quantum device design, IBM Research, 2021. [Online]. Available: `https://qiskit-community.github.io/qiskit-metal/`. [Accessed: 21-Sep-2024].

[4] "Ansys HFSS: High-Frequency Electromagnetic Field Simulator", Ansys Inc., 2021. [Online]. Available: `https://www.ansys.com/products/electronics/ansys-hfss`.

[5] Minev, Z. K., "pyEPR: Python for Energy Participation Ratio", GitHub Repository, 2021. [Online]. Available: `https://github.com/zlatko-minev/pyEPR`.

[6] Google Drive, "Research Materials", [Online]. Available: `https://drive.google.com/drive/folders/191m9DIh21H3wqIjl6iZJW8_BW2BCVQdK`. [Accessed: 21-Sep-2024].

[7] U. Mathur, "Research Data," Google Drive Folder, Accessed: Sep. 21, 2024. [Online]. Available: `https://drive.google.com/drive/folders/1M8SIWRY6tLHetKA8CHk7AQVbk6Us55JI`.

[8] Kuldeep Kumar Shrivastava et al., "Unveiling photon-photon coupling induced transparency and absorption", *Journal of Physics D: Applied Physics*, vol. 57, no. 46, pp. 465305, 2024. [Online]. Available: `https://iopscience.iop.org/article/10.1088/1361-6463/ad6613`. [Accessed: 21-Sep-2024].